PAPER

Nonlocal three-dimensional theory of elasticity for buckling behavior of functionally graded porous nanoplates using volume integrals

To cite this article: Mohammad Malikan *et al* 2018 *Mater. Res. Express* **5** 095006

View the article online for updates and enhancements.

Materials Research Express

CrossMark

Nonlocal three-dimensional theory of elasticity for buckling behavior of functionally graded porous nanoplates using volume integrals

Mohammad Malikan[1,4] , Francesco Tornabene[2] and Rossana Dimitri[3]

1   Department of Mechanical Engineering, Faculty of Engineering, Islamic Azad University, Mashhad Branch, Mashhad, Iran
2   Department of Civil, Chemical, Environmental, and Materials Engineering, University of Bologna, Bologna, Italy
3   Department of Innovation Engineering, University of Salento, Lecce, Italy
4   Author to whom any correspondence should be addressed.

E-mail: mohammad.malikan@yahoo.com, francesco.tornabene@unibo.it and rossana.dimitri@unisalento.it

Abstract

In this paper, the buckling of rectangular functionally graded (FG) porous nanoplates based on three-dimensional elasticity is investigated. Since, similar researches have been done in two-dimensional analyses in which only large deflections with constant thickness were studied by using various plate theories; therefore, discussion of large deformations and change in thickness of plates after deflection in this study is examined. Moreover, porosity is assumed in two situations, even and uneven distributions considered in several conditions. Using nonlocal elasticity theory, nonlocal three-dimensional equations are obtained. Regarding difficulties in solving three-dimensional differential equations, simple analytical methods are assumed and proposed. The most important results show that even porosity makes the plate softer and results of uneven porosity are so close to the prefect material which leads to this considerable conclusion that porosity as an uneven distribution cannot be an important factor in static stability analyses of FG nanoplates.

1. Introduction

Plates are important elements included in industrial machines and engineering structures that may miss their stability under tensile, compressive and shearing loads. The minimum stableness force is a remarkable quantity in engineering design and simulation. Todays, the combinatorial applications of materials are becoming more and more widespread in order to obtain appropriate properties. Given the advancement of technology, a material cannot, by itself, be responsive to advanced industry's needs. So, to satisfy such a request, the laminated functionally composite materials were produced which had two entirely different properties in their opposite surfaces. However, they were not suitable in light of the fact that these materials were layered because of residual stresses which led to their short life. Therefore, the non-homogenous materials have been produced within which their microstructural mechanical properties gradually change from a surface to another one. Due to lack of sudden split in these materials against laminated composites, their resistance were improved noticeably and also the stresses were distributed uniformly because of removing stress concentration. In this regard, study of the critical conditions of such materials is a serious need. Lee *et al* [1] used a mesh-free radial interpolation approach for examining nonlinear stability of functionally graded (FG) plates subjected to thermal in-plane loads. Lieu *et al* [2] taken a FG variable thickness plate for free vibration and bending responses. They assumed functionally graded property in bi-directional and solved the harvested equations by an isogeometric technic. Thai and Kim [3] analyzed resonant frequencies and bending of a FG plate by proposing a simple higher-order shear deformation theory. Ohadi *et al* [4] considered nonlinear thermo-vibrational behavior of a FG plate with taken piezoelectric layers. Zenkour and Radwan [5] compressively studied a FG plate embedded on an elastic foundation. They used a refined shear deformation theory with choosing a hyperbolic function rather than using shear correction factors. They also used an analytical solution from which various boundary conditions were accurately obtained in order to calculate maximum deflections. Thai and Vo [6] derived a new sinusoidal shear

deformation theory for static and dynamic analyses of FG plates based on the Navier approach. Wang *et al* [7] investigated stability of a FG thin plate with assuming in-plane material inhomogeneity. Thai and Kim [8] employed a closed-form solution for stability analysis of thick FG plates rested on a polymer matrix. They used third-order shear deformation theory in order to derive the equilibrium equations. The equations were solved by applying Levy solution for simply-supported boundary conditions. Bever and Duwez [9] considered gradients in the structure of composite materials to exhibit their compositional properties. Carrera *et al* [10] evaluated thickness stretching influences in single and multi-layered FG plates and shells. With regard to the Carrera's unified formulation, variable plate/shell theories were implemented. Bousahla *et al* [11] analyzed buckling of FG plates on the basis of a modified four-variable plate model exposed to linear and non-linear temperature distributions in the thickness direction. Akavci [12] studied stability and resonant frequencies of a FG composite plate rested on a soft foundation by proposing a new shear deformation theory in which a hyperbolic function was used instead of employing any shear correction factor. Bouderba *et al* [13] derived a simplified first-order theory of shear deformation in which only four-unknown variables were existed. This new plate theory was employed to examine a FG sandwich plate in a thermal buckling condition. Ghadiri *et al* [14] investigated for the first time influences of Coriolis and thermal on the natural frequency analysis of a FG plate which was in a rotational condition. To this, generalized differential quadrature method was applied for cantilever boundary conditions. El-Haina *et al* [15] proposed a new simple analytical solution technic in order to study stability of a thick FG composite plate subjected to thermal in-plane forces. Hichem *et al* [16] derived a simple and efficient four-variable shear deformation theory to study elastic stability of a FG plate.

On the other hand, in recent years, due to developing of the use of engineering structures in small-scale and necessity to optimize their performance, researchers have been encouraged to use materials with micro and nanoscales. Liu *et al* [17] investigated wave propagation in nanoplates with considering piezoelectricity influences. They also considered surface piezoelectricity and nonlocal impacts in their research. Li *et al* [18] in a special work modeled flexural wave propagation for a nonlocal FG beam using nonlocal strain gradient theory. Shahsavari and Janghorban [19] dynamically analyzed the shearing and bending response of a graphene plate under a concentrated moving load. A two-variable shear deformation theory was accompanied with nonlocal elasticity theory of Eringen in order to derive the vibrational equations and the obtained relations were calculated with Navier technic. Hichem *et al* [20] formulated a zeroth-order shear deformation theory and applied it for examining post-stability of a nanoscale beam. Eringen's law and a closed-form approach were employed to achieve this aim. A wave propagation analysis for double-walled carbon nano shell models was investigated by Tadi Beni *et al* [21]. They modeled a slip boundary condition and assumed that the nanotube conveys fluid. To consider nanoscale properties, nonlocal strain gradient theory was used and the model was surrounded in a polymer matrix. Janghorban *et al* [22] employed a novel higher-order nonlocal strain gradient shell theory for analytically studying wave dispersion in a doubly-curved nano shell. The mechanical behavior of the model was assumed to be an anisotropic shell. In a specific research, Karami *et al* [23] employed three-dimensional elasticity formulation for considering a FG nano spherical model. They applied small-scale effects with using nonlocal strain gradient theory and incorporated the anisotropic property for the model. Ebrahimi and Salari [24] analyzed natural frequencies and static stability of functionally graded (FG) nanobeams which were under in-plane thermal forces. The beam was modeled as a Timoshenko beam and nonlocality was modeled by nonlocal elasticity theory of Eringen. Tadi Beni *et al* [25] investigated stability of FG nano bridges under electro-mechanical in-plane loads with utilizing theory of strain gradient. Zamani Nejad *et al* [26] studied stability of FG nonlocal beams. They applied Euler–Bernoulli beams and presented a solution by taking into account the variation of properties in two-directional FG materials with arbitrary functions. They solved the equations with using generalized differential quadrature method for different boundary conditions. Yang *et al* [27] demonstrated thermal stability and post-stability of nano-FG composite plates.

In special analyses, various boundary conditions were considered. Akhavan *et al* [28] investigated the fundamental frequencies of a moderately thick FG plate with utilizing first-order theory of shear deformation. The plate was placed on a Winkler-Pasternak substrate and the derived equations were solved by an analytic assumption. Panda *et al* [29] studied stability of a FG single/doubly shell panel with initial curvature under thermal in-plane loads by considering temperature-dependent (TD) and temperature-independent (TID) properties. Abdelaziz *et al* [30] presented a new hyperbolic shear defirmation plate theory for analyzing functionally graded sandwich plates. They studied stability, bending and natural frequencies of the composite plate whilst several boundary conditions were applied. Many articles have also been presented in recent years in terms of FGMs and nano materials [31–64].

In addition to these, the materials with porosity are another type of materials with different behavior [65]. The nanoporous materials have cavities in nanoscale which are diverse. In fact, the volumetric ratio of cavity of the porous material to the total volume is called the porosity [66–68]. According to the definition of nanotechnology, chemistry scientists use nanoporous for materials that contain cavities with a diameter of less than 100 nm [66–68]. In terms of such materials, Shafiei and Kazemi [69] carried out the nonlinear stability of
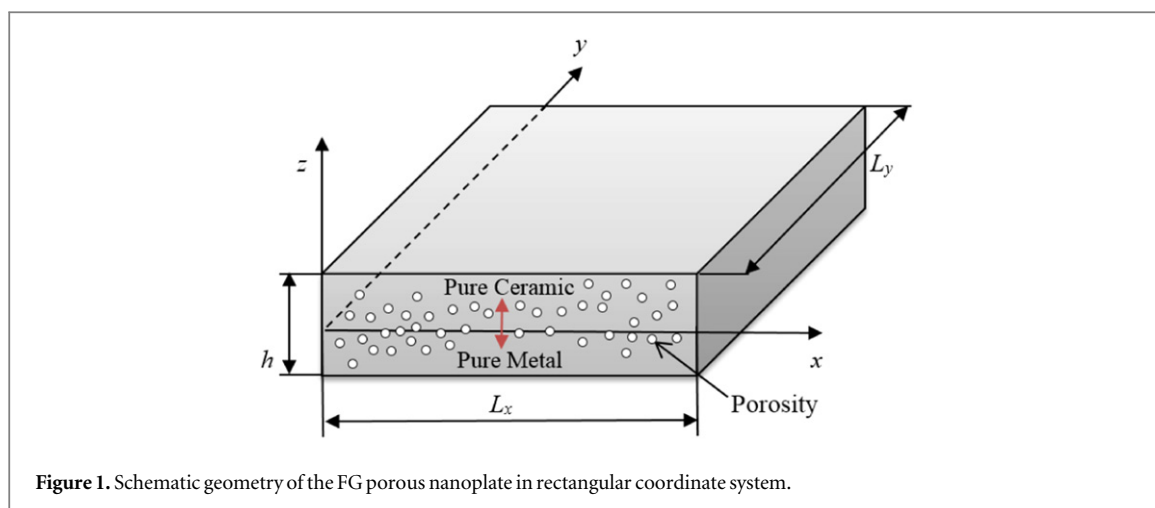
Figure 1. Schematic geometry of the FG porous nanoplate in rectangular coordinate system.

micro/nano functionally graded (FG) porous beams. Wang and Zu [70] studied vibrational responses of a FG non-square porous plate exposed to thermal in-plane forces. Resonant frequencies of FG porous plates with piezoelectricity impacts under electro-mechanical loads in a translation state was studied by Wang [71].

In view of exact analyses literature, there are a few research within which the materials have been analyzed three-dimensionally. Ansari *et al* [72] examined free vibration of functionally graded (FG) nanoplates on elastic foundations via three-dimensional theory of elasticity. The generalized differential quadrature method was adopted by using three-dimensional meshing. Brischetto [73] developed an exact three-dimensional equation for static analysis of single and multi-layered shells and plates. The equations were solved via a proposed exact 3D shell method by which simple boundary conditions were satisfied. The shell solution was based on a layer-wise approach and the second order differential equations were solved using the redouble of variables and the exponential matrix method. Ansari *et al* [74] three-dimensionally analyzed static and dynamic of FG nanoplates based on a new differential quadrature-based approach. They established nonlocal elasticity theory of Eringen to take into account nanoscale effects and it was found that the proposed approach had a fast rate of convergence. Dastjerdi and Akgöz [75] conducted new static and dynamic models of nano and macro FG plates based on the three-dimensional elasticity by considering thermal effects. Their results showed that if the thermal analysis is considered, neglecting the amount of ε_{zz} leads to serious errors, and only the results of the three-dimensional elasticity theory should be used. Nahvi *et al* [76] presented three-dimensional elasticity formulation for bending behavior of FG micro/nanoplates placed on an elastic medium on the basis of a couple stress approach and an analytical solution. Three-dimensional thermo-elastic solution of a composite plate with a FG core under thermal shock using Fourier series expansion was investigated by Alibeigloo [77]. Kant *et al* [78] compared the three-dimensional elasticity solutions for FG plates. The Pagano's classical, series expansion, mixed formulation, state space and semi analytical approaches were compared to one another.

In this paper, it is aimed to three-dimensionally analyze the mechanical behavior of a porous functionally graded nanoplate under critical stability conditions to have a more accurate model. The governing equations are derived based on the Eringen's nonlocal elasticity theory with taking porosities effects into consideration. To solve the achieved equations, a proposed analytical method is presented by employing some suitable shape functions. The proposed volume integral is a simple method in contrast to the solution techniques in the literature. In order to verify the outcomes of the equations, the results of three-dimensional analysis are compared with results of plate theories. Afterwards, the results of the current analysis are plotted by investigating several parameters such as power law, porosity factor, thickness to length ratio, nonlocal parameter and aspect ratio.

2. Mathematical modeling

A rectangular FG nanoplate is shown in figure 1. The development of nanotechnologies extends the field of application of the classical or non-classical theories of plates. Recently, many theories of nanoscale have been suggested and various theories of plates are formulated. The classical plate theory (CPT) is inconsistent in the sense that elements are assumed to remain perpendicular to the mid-plane, yet equilibrium requires that stress components σ_{xz}, σ_{yz} still arise (which would cause these elements to deform). The theory of thick plates (higher-order transverse shear deformation theories (HSDT) or third-order shear deformation theory (TSDT)) are more appropriate, but they still make the assumption that $\sigma_z = 0$. Note that both are approximations of the

three-dimensional equations of elasticity. Hence, in this study, by considering changes in thickness of the plate the three-dimensional elasticity relations are presented. In this regard, general three-dimensional displacement field can be expressed as [75]:

$$U(x, y, z, t) = u(x, y, z) \tag{1a}$$

$$V(x, y, z, t) = v(x, y, z) \tag{1b}$$

$$W(x, y, z, t) = w(x, y, z) \tag{1c}$$

In which u, v and w are the three-dimensional displacement parameters regarding the x, y and z-axis. The three-dimensional constitutive model is the most general type of material models considered in this paper. The non-zero stiffness coefficients of the stiffness matrix are defined as follows [75]:

$$[Q_{ijkl}]$$
$$= \begin{bmatrix} \dfrac{E(z)(1 - \nu(z))}{K} & \dfrac{E(z)\nu(z)}{K} & \dfrac{E(z)\nu(z)}{K} & 0 & 0 & 0 \\[2mm] \dfrac{E(z)\nu(z)}{K} & \dfrac{E(z)(1 - \nu(z))}{K} & \dfrac{E(z)\nu(z)}{K} & 0 & 0 & 0 \\[2mm] \dfrac{E(z)\nu(z)}{K} & \dfrac{E(z)\nu(z)}{K} & \dfrac{E(z)(1 - \nu(z))}{K} & 0 & 0 & 0 \\[2mm] 0 & 0 & 0 & \dfrac{E(z)}{2(1 + \nu(z))} & 0 & 0 \\[2mm] 0 & 0 & 0 & 0 & \dfrac{E(z)}{2(1 + \nu(z))} & 0 \\[2mm] 0 & 0 & 0 & 0 & 0 & \dfrac{E(z)}{2(1 + \nu(z))} \end{bmatrix} \tag{2}$$

$$K = (1 + \nu(z))(1 - 2\nu(z)) \tag{3}$$

The material property gradation considering power law in the FG nanoplates is expressed as [74–76]:

$$E(z) = E_m + (E_c - E_m)\left(\frac{1}{2} + \frac{z}{h}\right)^k \tag{4}$$

Here E shows the modulus of elasticity, h represent the thickness of the plate before deflection, E_c and E_m are the Young's modulus corresponding to ceramic and metal, respectively, and k is volume fraction exponent or material grading/power law index. Due to insignificant variation of the Poisson's ratio, this variant is assumed to be constant along the thickness ($\nu(z) = \nu$). From equation (4), whenever $k \to \infty$, the FG nanoplate reduces to a pure metal and for case $k = 0$, the plate would be a pure ceramic.

According to equation (4) and using a porosity distribution type [79], the physical and mechanical properties of the FG porous nanoplate is as follows:

$$E(z) = E_m + (E_c - E_m)\left(\frac{1}{2} + \frac{z}{h}\right)^k - \frac{\alpha}{2}(E_c + E_m) \tag{5a}$$

$$E(z) = E_m + (E_c - E_m)\left(\frac{1}{2} + \frac{z}{h}\right)^k - \frac{\alpha}{2}(E_c + E_m)\left(1 - \frac{2|z|}{h}\right) \tag{5b}$$

where α is the porosity distribution factor. Equation (5a) shows evenly distributed porosities (P-I) and equation (5b) represents unevenly distributed porosities (P-II) [80]. Thereafter, the Lagrangian strains are:

$$\varepsilon_{ij} = \frac{1}{2}\left(\frac{\partial u_i}{\partial x_j} + \frac{\partial u_j}{\partial x_i} + \frac{\partial u_k}{\partial x_i}\frac{\partial u_k}{\partial x_j}\right), \quad i, j, k = x, y, z \tag{6}$$

where $\sigma_{ij}(i = x, y, z)$ is the static stresses in the plate. Using equation (6) and with considering the von Kármán assumption the three-dimensional strains field are expressed as follows:

$$
\begin{Bmatrix} \varepsilon_{xx} \\ \varepsilon_{yy} \\ \varepsilon_{zz} \\ \gamma_{xz} \\ \gamma_{yz} \\ \gamma_{xy} \end{Bmatrix} = \begin{bmatrix} \dfrac{\partial u}{\partial x} + \dfrac{1}{2}\left(\dfrac{\partial w}{\partial x}\right)^2 \\[2mm] \dfrac{\partial v}{\partial y} + \dfrac{1}{2}\left(\dfrac{\partial w}{\partial y}\right)^2 \\[2mm] \dfrac{\partial w}{\partial z} + \dfrac{1}{2}\left(\dfrac{\partial w}{\partial z}\right)^2 \\[2mm] \dfrac{\partial u}{\partial z} + \dfrac{\partial w}{\partial x}\left(\dfrac{\partial w}{\partial z} + 1\right) \\[2mm] \dfrac{\partial v}{\partial z} + \dfrac{\partial w}{\partial y}\left(\dfrac{\partial w}{\partial z} + 1\right) \\[2mm] \dfrac{\partial u}{\partial y} + \dfrac{\partial v}{\partial x} + \dfrac{\partial w}{\partial x}\dfrac{\partial w}{\partial y} \end{bmatrix}
\tag{7}
$$

To obtain the total potential energy (V) of the plate, strain energy is added to the potential energy of external loads as follows [81]:

$$
V = U + \Omega
\tag{8}
$$

where U is the strain energy as follows:

$$
\delta U = \iiint_v \sigma_{ij}^{NONLOCAL}\, \delta\, \varepsilon_{ij} dV,\ i, j = x, y, z
\tag{9}
$$

And Ω is the potential energy of external loads neglected in this paper.

Using the principle of minimum total potential energy ($\delta V = 0$) the nonlinear three-dimensional governing equations are obtained in the following equations:

$$
\delta u = 0: \frac{\partial \sigma_x^{NL}}{\partial x} + \frac{\partial \sigma_{xy}^{NL}}{\partial y} + \frac{\partial \sigma_{xz}^{NL}}{\partial z} = 0
\tag{10a}
$$

$$
\delta v = 0: \frac{\partial \sigma_{xy}^{NL}}{\partial x} + \frac{\partial \sigma_y^{NL}}{\partial y} + \frac{\partial \sigma_{yz}^{NL}}{\partial z} = 0
\tag{10b}
$$

$$
\delta w = 0: \frac{\partial \sigma_{xz}^{NL}}{\partial x}\left(1 + \frac{\partial w}{\partial z}\right) + \frac{\partial \sigma_{xz}^{NL}}{\partial z}\frac{\partial w}{\partial x} + \frac{\partial \sigma_{yz}^{NL}}{\partial y}\left(1 + \frac{\partial w}{\partial z}\right) + \frac{\partial \sigma_{yz}^{NL}}{\partial z}\frac{\partial w}{\partial y} + 2\sigma_{xz}^{NL}\frac{\partial^2 w}{\partial x \partial z} + 2\sigma_{yz}^{NL}\frac{\partial^2 w}{\partial y \partial z}
$$
$$
+ \sigma_x^{NL}\frac{\partial^2 w}{\partial x^2} + \sigma_y^{NL}\frac{\partial^2 w}{\partial y^2} + 2\sigma_{xy}^{NL}\frac{\partial^2 w}{\partial x \partial y} + \sigma_z^{NL}\frac{\partial^2 w}{\partial z^2} + \frac{\partial \sigma_z^{NL}}{\partial z}\left(1 + \frac{\partial w}{\partial z}\right) = 0
\tag{10c}
$$

In which subscript *NL* and *L* denote the quantities for the Nonlocal and Local cases, respectively. The local and nonlocal stress-displacement relations are defined as [82, 83]:

$$
(1 - \mu\nabla^2)\sigma_{ij}^{NONLOCAL} = \sigma_{ij}^{LOCAL}, \quad \mu = (e_0 a)^2, \quad \nabla^2 = \frac{\partial^2}{\partial x^2} + \frac{\partial^2}{\partial y^2} + \frac{\partial^2}{\partial z^2}
\tag{11}
$$

Using equation (11) and substituting it into equation (10), the nonlocal three-dimensional equations with local stresses are obtained as follows:

$$
\frac{\partial \sigma_x^L}{\partial x} + \frac{\partial \sigma_{xy}^L}{\partial y} + \frac{\partial \sigma_{xz}^L}{\partial z} = 0
\tag{12a}
$$

$$
\frac{\partial \sigma_{xy}^L}{\partial x} + \frac{\partial \sigma_y^L}{\partial y} + \frac{\partial \sigma_{yz}^L}{\partial z} = 0
\tag{12b}
$$

$$\frac{\partial \sigma_{xz}^L}{\partial x} + \frac{\partial \sigma_{yz}^L}{\partial y} + \frac{\partial \sigma_z^L}{\partial z} + \left[\sigma_x^L \frac{\partial^2 w}{\partial x^2} + \sigma_y^L \frac{\partial^2 w}{\partial y^2} + \sigma_z^L \frac{\partial^2 w}{\partial z^2} + 2\sigma_{xy}^L \frac{\partial^2 w}{\partial x \partial y} + 2\sigma_{xz}^L \frac{\partial^2 w}{\partial x \partial z} + 2\sigma_{yz}^L \frac{\partial^2 w}{\partial y \partial z} \right.$$

$$\left. + \frac{\partial \sigma_{xz}^L}{\partial z}\frac{\partial w}{\partial x} + \frac{\partial \sigma_{xz}^L}{\partial x}\frac{\partial w}{\partial z} + \frac{\partial \sigma_{yz}^L}{\partial y}\frac{\partial w}{\partial z} + \frac{\partial \sigma_{yz}^L}{\partial z}\frac{\partial w}{\partial y} + \frac{\partial \sigma_z^L}{\partial z}\frac{\partial w}{\partial z} \right] - \mu \left(\frac{\partial^2 w}{\partial x^2} + \frac{\partial^2 w}{\partial y^2} + \frac{\partial^2 w}{\partial z^2} \right)$$

$$\times \left[\sigma_x^L \frac{\partial^2 w}{\partial x^2} + \sigma_y^L \frac{\partial^2 w}{\partial y^2} + \sigma_z^L \frac{\partial^2 w}{\partial z^2} + 2\sigma_{xy}^L \frac{\partial^2 w}{\partial x \partial y} + 2\sigma_{xz}^L \frac{\partial^2 w}{\partial x \partial z} + 2\sigma_{yz}^L \frac{\partial^2 w}{\partial y \partial z} + \frac{\partial \sigma_{xz}^L}{\partial z}\frac{\partial w}{\partial x} \right.$$

$$\left. + \frac{\partial \sigma_{xz}^L}{\partial x}\frac{\partial w}{\partial z} + \frac{\partial \sigma_{yz}^L}{\partial y}\frac{\partial w}{\partial z} + \frac{\partial \sigma_{yz}^L}{\partial z}\frac{\partial w}{\partial y} + \frac{\partial \sigma_z^L}{\partial z}\frac{\partial w}{\partial z} \right] = 0 \tag{12c}$$

Now by writing the relation of stresses and strains and helping equation (7) the stress field is expressed:

$$
\begin{Bmatrix} \sigma_{xx} \\ \sigma_{yy} \\ \sigma_{zz} \\ \sigma_{xz} \\ \sigma_{yz} \\ \sigma_{xy} \end{Bmatrix}
=
\begin{bmatrix}
\frac{E(z)(1-\nu(z))}{K} & \frac{E(z)\nu(z)}{K} & \frac{E(z)\nu(z)}{K} & 0 & 0 & 0 \\[2mm]
\frac{E(z)\nu(z)}{K} & \frac{E(z)(1-\nu(z))}{K} & \frac{E(z)\nu(z)}{K} & 0 & 0 & 0 \\[2mm]
\frac{E(z)\nu(z)}{K} & \frac{E(z)\nu(z)}{K} & \frac{E(z)(1-\nu(z))}{K} & 0 & 0 & 0 \\[2mm]
0 & 0 & 0 & \frac{E(z)}{2(1+\nu(z))} & 0 & 0 \\[2mm]
0 & 0 & 0 & 0 & \frac{E(z)}{2(1+\nu(z))} & 0 \\[2mm]
0 & 0 & 0 & 0 & 0 & \frac{E(z)}{2(1+\nu(z))}
\end{bmatrix}
$$

$$
\times
\begin{Bmatrix}
\frac{\partial u}{\partial x} + \frac{1}{2}\left(\frac{\partial w}{\partial x}\right)^2 \\[2mm]
\frac{\partial v}{\partial y} + \frac{1}{2}\left(\frac{\partial w}{\partial y}\right)^2 \\[2mm]
\frac{\partial w}{\partial z} + \frac{1}{2}\left(\frac{\partial w}{\partial z}\right)^2 \\[2mm]
\frac{\partial u}{\partial z} + \frac{\partial w}{\partial x}\left(\frac{\partial w}{\partial z} + 1\right) \\[2mm]
\frac{\partial v}{\partial z} + \frac{\partial w}{\partial y}\left(\frac{\partial w}{\partial z} + 1\right) \\[2mm]
\left(\frac{\partial u}{\partial y} + \frac{\partial v}{\partial x}\right) + \frac{\partial w}{\partial x}\frac{\partial w}{\partial y}
\end{Bmatrix}
\tag{13}
$$

Due to the fact that the nonlinear terms in equation (13) are very small and there is no need to use them, in particular in stability analysis; therefore, they should be ignored. On the other hand, substituting equation (13) into equation (12) and also using the adjacent equilibrium method, the nonlocal three-dimensional equations in the displacement field are obtained as follows:

$$\frac{E(z)(1-\nu(z))}{K}\frac{\partial^2 u}{\partial x^2} + \frac{E(z)\nu(z)}{K}\frac{\partial^2 v}{\partial x \partial y} + \frac{E(z)}{2(1+\nu(z))}\left(\frac{\partial^2 u}{\partial y^2} + \frac{\partial^2 v}{\partial x \partial y} + \frac{\partial^2 u}{\partial z^2} + \frac{\partial^2 w}{\partial x \partial z} \right) = 0 \tag{14a}$$

$$\frac{E(z)\nu(z)}{K}\frac{\partial^2 u}{\partial x \partial y} + \frac{E(z)(1-\nu(z))}{K}\frac{\partial^2 v}{\partial y^2} + \frac{E(z)}{2(1+\nu(z))}\left(\frac{\partial^2 u}{\partial x \partial y} + \frac{\partial^2 v}{\partial x^2} + \frac{\partial^2 v}{\partial z^2} + \frac{\partial^2 w}{\partial y \partial z} \right) = 0 \tag{14b}$$

Table 1. Admissible functions assumed solutions in the directions.

Displacements	SS-I		SS-II		
	$X_m(x)$	$Y_n(y)$	$X_m(x)$	$Y_n(y)$	$Z_r(z)$
$u(x, y, z)$	$\mathrm{Cos}\left(\dfrac{m\pi}{L_x}x\right)$	$\mathrm{Sin}\left(\dfrac{n\pi}{L_y}y\right)$	$\dfrac{\partial\left(\mathrm{Cos}\left(\dfrac{m\pi}{L_x}x\right)\right)}{\partial x}$	$\mathrm{Sin}\left(\dfrac{n\pi}{L_y}y\right)$	$Z_1(z): z\left[1-\dfrac{4z^2}{3h^2}\right]$
$v(x, y, z)$	$\mathrm{Sin}\left(\dfrac{m\pi}{L_x}x\right)$	$\mathrm{Cos}\left(\dfrac{n\pi}{L_y}y\right)$	$\mathrm{Sin}\left(\dfrac{m\pi}{L_x}x\right)$	$\dfrac{\partial\left(\mathrm{Cos}\left(\dfrac{n\pi}{L_y}y\right)\right)}{\partial y}$	$Z_2(z): \sin\left(\dfrac{\pi z}{h}\right)$
$w(x, y, z)$	$\mathrm{Sin}\left(\dfrac{m\pi}{L_x}x\right)$	$\mathrm{Sin}\left(\dfrac{n\pi}{L_y}y\right)$	$\mathrm{Sin}\left(\dfrac{m\pi}{L_x}x\right)$	$\mathrm{Sin}\left(\dfrac{n\pi}{L_y}y\right)$	$Z_3(z): \cos\left(\dfrac{\pi z}{h}\right)$

$$\frac{E(z)}{2(1+\nu(z))}\left(\frac{\partial^2 u}{\partial x \partial z}+\frac{\partial^2 w}{\partial x^2}+\frac{\partial^2 v}{\partial y \partial z}+\frac{\partial^2 w}{\partial y^2}\right)+\frac{E(z)(1-\nu(z))}{K}\frac{\partial^2 w}{\partial z^2}+\sigma_x^L\frac{\partial^2 w}{\partial x^2}+\sigma_y^L\frac{\partial^2 w}{\partial y^2}$$

$$-\mu\left(\sigma_x^L\left(\frac{\partial^4 w}{\partial x^4}+\frac{\partial^4 w}{\partial x^2 \partial y^2}+\frac{\partial^4 w}{\partial x^2 \partial z^2}\right)+\sigma_y^L\left(\frac{\partial^4 w}{\partial y^4}+\frac{\partial^4 w}{\partial x^2 \partial y^2}+\frac{\partial^4 w}{\partial y^2 \partial z^2}\right)\right)=0 \tag{14c}$$

3. Solution methodology

In order to complete the formulation, the stability equations (equation (14)) should be accompanied by a set of boundary conditions. Therefore, in this paper a type of boundary condition is applied. The type is the simply supported (S) boundary condition. Below is the case of this boundary condition [72]:

- Edge Boundary conditions
  All edges simply supported (SSSS):

$$v = w = \sigma_x = 0, \quad :x = 0, \; L_x$$
$$u = w = \sigma_y = 0, \quad :y = 0, \; L_y \tag{15}$$

- Surface Boundary conditions

  Since the nanoplate is considered in three dimensions, the surface boundary conditions are defined by:

$$\sigma_z = 0, \; \sigma_{xz} = 0, \; \sigma_{yz} = 0 : \; z = 0, \; h \tag{16}$$

To solve the stability equations, a method has been presented in which the responses are assumed to be as follows:

$$\begin{Bmatrix} u(x, y, z) \\ v(x, y, z) \\ w(x, y, z) \end{Bmatrix} = \sum_{m=1}^{\infty}\sum_{n=1}^{\infty}\begin{Bmatrix} A_{mnr}.X_m(x).Y_n(y).Z_r(z) \\ B_{mnr}.X_m(x).Y_n(y).Z_r(z) \\ C_{mnr}.X_m(x).Y_n(y).Z_r(z) \end{Bmatrix} \tag{17}$$

In which $X_m(x)$ and $Y_n(y)$ are admissible shape functions on the basis of x and y which satisfy the boundary conditions in equation (15), $Z_r(z)$ is the approximate solution in the direction of z-axis. And A_{mnr}, B_{mnr} and C_{mnr} are the constant coefficients which should be calculated. Note that the proposed solutions are approximations of the analytical method for three-dimensional equations. This means that by using the present solutions, the quasi three-dimensional analytical approaches have been applied. These are simpler than the other solutions which have been used to solve three-dimensional elasticity equations. In some references, the Navier solution was used as a three-dimensional exact method [84] which its relations are harder than the current formulation. The suitable shape functions are proposed in table 1.

Where m and n are the integer numbers. Substituting equation (17) into eqaution (14), a residual in the algebraic form will be obtained, based on the presented approach, the residual will be calculated by:

$$\iiint R(x, \; y, \; z).X_{m,n}(x, \; y).Z_r(z)\,dzdydx = 0, \; \text{m, n} = 1, \; 2, \; 3, \dots \tag{18}$$

On the basis of equation (18), the system of homogenous algebraic equations will be obtained as:

$$
\begin{bmatrix} K_{11} & K_{12} & K_{13} \\ K_{21} & K_{22} & K_{23} \\ K_{31} & K_{32} & K_{33} \end{bmatrix} \begin{Bmatrix} A_{mnr} \\ B_{mnr} \\ C_{mnr} \end{Bmatrix} = 0
\tag{19}
$$

where $(A, \ B, \ C)$ are the unknown variables. Also $[K_{ij}]$ are coefficients of unknown variables which are shown as follows:

$$
K_{11} = \int_0^{Lx} \int_0^{Ly} \int_0^h \left(\frac{E(z)(1-\nu(z))}{K} \frac{\partial^2 X_m}{\partial x^2} X_n X_r + \frac{E(z)}{2(1+\nu(z))} \left(\frac{\partial^2 X_n}{\partial y^2} X_m X_r + \frac{\partial^2 X_r}{\partial z^2} X_m X_n \right) \right)
$$
$$
\times X_m X_n X_r \, dz dy dx
$$

$$
K_{12} = \int_0^{Lx} \int_0^{Ly} \int_0^h \left(\frac{E(z)\nu(z)}{K} + \frac{E(z)}{2(1+\nu(z))} \right) \frac{\partial^2 X_n}{\partial x \partial y} X_m{}^2 X_n X_r{}^2 dz dy dx
$$

$$
K_{13} = \int_0^{Lx} \int_0^{Ly} \int_0^h \frac{E(z)}{2(1+\nu(z))} \frac{\partial^2 X_{m,r}}{\partial x \partial z} X_m X_n{}^2 X_r \, dz dy dx
$$

$$
K_{21} = \int_0^{Lx} \int_0^{Ly} \int_0^h \left(\frac{E(z)\nu(z)}{K} + \frac{E(z)}{2(1+\nu(z))} \right) \frac{\partial^2 X_{m,n}}{\partial x \partial y} X_m X_n X_r{}^2 dz dy dx
$$

$$
K_{22} = \int_0^{Lx} \int_0^{Ly} \int_0^h \left(\frac{E(z)(1-\nu(z))}{K} \frac{\partial^2 X_n}{\partial y^2} X_m X_r + \frac{E(z)}{2(1+\nu(z))} \left(\frac{\partial^2 X_m}{\partial x^2} X_n X_r + \frac{\partial^2 X_r}{\partial z^2} X_m X_r \right) \right)
$$
$$
\times X_m X_n X_r \, dz dy dx
$$

$$
K_{23} = \int_0^{Lx} \int_0^{Ly} \int_0^h \frac{E(z)}{2(1+\nu(z))} \frac{\partial^2 X_{n,r}}{\partial y \partial z} X_m{}^2 X_n X_r \, dz dy dx
$$

$$
K_{31} = \int_0^{Lx} \int_0^{Ly} \int_0^h \frac{E(z)}{2(1+\nu(z))} \frac{\partial^2 X_{m,r}}{\partial x \partial z} X_m X_n{}^2 X_r \, dz dy dx
$$

$$
K_{32} = \int_0^{Lx} \int_0^{Ly} \int_0^h \frac{E(z)}{2(1+\nu(z))} \frac{\partial^2 X_{n,r}}{\partial y \partial z} X_m{}^2 X_n X_r \, dz dy dx
$$

$$
K_{33} = \int_0^{Lx} \int_0^{Ly} \int_0^h \left[\frac{E(z)}{2(1+\nu(z))} \left(\frac{\partial^2 X_m}{\partial x^2} X_n X_r + \frac{\partial^2 X_n}{\partial y^2} X_m X_r \right) + \frac{E(z)(1-\nu(z))}{K} \frac{\partial^2 X_r}{\partial z^2} X_m X_n \right.
$$
$$
+ \sigma_x^L \frac{\partial^2 X_m}{\partial x^2} X_n X_r + \sigma_y^L \frac{\partial^2 X_n}{\partial y^2} X_m X_r - \mu \left(\sigma_x^L \left(\frac{\partial^4 X_m}{\partial x^4} X_n X_r + \frac{\partial^4 X_{m,n}}{\partial x^2 \partial y^2} X_r + \frac{\partial^4 X_{m,r}}{\partial x^2 \partial z^2} X_n \right) \right.
$$
$$
\left. \left. + \sigma_y^L \left(\frac{\partial^4 X_n}{\partial y^4} X_m X_r + \frac{\partial^4 X_{m,n}}{\partial x^2 \partial y^2} X_r + \frac{\partial^4 X_{n,r}}{\partial y^2 \partial z^2} X_m \right) \right) \right] X_m X_n X_r \, dz dy dx
\tag{20}
$$

4. Results and discussions

In this section, several comparisons for some materials and conditions in order to determine the precision of the proposed analytical solution are carried out. First of all, buckling of uniaxially compressed rectangular isotropic macro plates is considered while all the edges are simple boundaries. Results are shown from [85] in which exact three-dimensional theory of elasticity was used in conjunction with differential quadrature and hyperbolic differential quadrature methods, (DQ) and (HDQ). Moreover, Mindlin plate theory was accompanied with Pb-Ritz method in [86]. It can be seen that the results decreased with increasing thickness to length ratio (span ratio). As can be observed, the distance among the results of the current paper and [85] with those obtained by ref [86] with increasing span ratio is jumped remarkably. However with increasing aspect ratio these distances have become further smaller and it can be found that plate theories in analyzing rectangular plates with large length have further accurate results than square ones. This might be because of shortcoming of plate theories to analyze moderately thick and thick plates which means that assuming constant thickness after deflection in plate theories can be a serious weakness. Table 2 is similar to previous table, but here the results are verified with biaxial buckling of the plate. It is worth noting that within biaxial analysis, the deviation of the Mindlin plate theory is lesser in contrast to table 1 and then also the results of present paper are closer to [85] against former table. Another comparison is taken into consideration with [87] and [88] in which equations of first-order shear deformation theory (FSDT) were solved with DQ and

Table 2. Comparison of buckling factors, $\lambda = N_x Ly^2 h / \pi^2 D \,(D = Eh^3/12(1-\nu^2))$, of the uniaxially compressed rectangular plates.

Boundary conditions	Aspect ratio (Lx/Ly) Grid size, $X \times Y \times Z$	Thickness to width ratio, h/Ly								
		0.05			0.10			0.15		
		[85] 3D, HDQ DQ	[86] Mindlin, Pb-Ritz method	Present, 3D	[85] 3D, HDQ DQ	[86] Mindlin, Pb-Ritz method	Present, 3D	[85] 3D, HDQ DQ	[86] Mindlin, Pb-Ritz method	Present, 3D
SSSS	0.5	5.8107 5.9899	6.0346	6.0204	5.3002 5.3412	5.4693	5.3529	8.2533 4.5530	4.7305	4.5607
	1.0	3.6387 3.9314	3.9437	3.9575	3.6709 3.7412	3.7839	3.7683	3.4382 3.4676	3.5446	3.4725
	1.5	4.0103 4.2375	4.2559	4.2120	3.9075 3.9613	4.0214	3.9369	3.5606 3.5827	3.6831	3.5520

*The results for HDQ and DQ are in convergence values.

then Mindlin plate theory were calculated with Pb-Ritz method, respectively. This table confirms this fact that when the plate is thicker, three-dimensional elasticity outcomes are farther than those results obtained by various plate theories. Additionally, to have more validation, table 5 is presented. In this table, a simply-supported square FG plate is considered. In other words, other than macro plates shown in tables 2 to 4, it is required to compare the results of current work with a FG plate. Again [87] is employed besides [89] within which the equations of an approximate plate theory were solved by Navier approach. When $k = 0$, present research and other references are in greatest difference to one another. It shows that by an increase in power law index, the results are in a good agreement, not only for present research, even for [89]. This needs to further consideration, for which tables 6 and 7 are demonstrated. It should be noted that the results of $h/L_x = 0.2$ are farther for three cases in contrast to $h/L_y = 0.1$. In table 6, a FG plate is analyzed by incorporating higher-order transverse shear deformation plate theory (HSDT) and solving with Levy [90] and also Navier [91] solution methods. Undoubtedly, one of the appropriate plate theories for evaluating moderately thick and thick plates can be HSDT applied in many papers over the past two decades. For $k = 1$, results are more satisfactorily acceptable with those references, however by decreasing this index, the values are found to be in a high percent difference from present paper to results given by [90, 91]. As a matter of fact, if the plate is thicker, the grading factor is more effective and makes the further distances in results of various solutions. It is worth mentioning that by using HSDT and increasing power law index the results originated from [90, 91] are becoming closer to each other in table 6, and by using thicker plates, the results of [87–89] are getting farther to each other in table 5. On the other hand, these effects are steady for present equations with HSDT which leads to closing results by an increase in k. This proves that the plate theories (CPT, FSDT, etc) cannot exactly predict the responses of thick and even moderately thick plates and it is better to use thick plate theories such as HSDT and TSDT. Finally, all of these harvests can be confirmed by the last one table. In table 7 the third-order shear deformation theory (TSDT) was applied [16] which is an accurate thick plate theory. It is obvious that the results lead to further matching with increasing material grading index and also length to thickness ratio. This conclusion is seen reversely in table 5 for plate theories which means that in thick plates, the thick plate theories such as HSDT, TSDT and etc can be fit ones in contrast to plate theories.

Tables	Quantities
tables 2 & 3	$E = 210$ GPa, $\nu = 0.3$ [85] $E = 210$ GPa, $\nu = 0.3$, $k_s = 5/6$ [86] $E = 210$ GPa, $\nu = 0.3$, $k = 0$, $\alpha = 0$ [Present]
table 4	$E = 3 \times 10^6$, $\nu = 0.3$, $k_s = 5/6$, $SSSS$ [87, 88] $E = 3 \times 10^6$, $\nu = 0.3$, $k = 0$, $\alpha = 0$, $SSSS$ [Present]
table 5	$E_m = 70$ GPa, $E_c = 380$ GPa, $\nu = 0.3$, $k_s = 5/6$ [87] $E_m = 70$ GPa, $E_c = 380$ GPa, $\nu = 0.3$ [89] $E_m = 70$ GPa, $E_c = 380$ GPa, $\nu = 0.3$, $\alpha = 0$ [Present]
table 6	$E_m = 70$ GPa, $E_c = 420$ GPa, $\nu = 0.3$, $h/L_y = 0.1$ [90, 91] $E_m = 70$ GPa, $E_c = 420$ GPa, $\nu = 0.3$, $\alpha = 0$, $h/L_y = 0.1$ [Present]
table 7	$E_m = 70$ GPa, $E_c = 380$ GPa, $\nu = 0.3$, [16] $E_m = 70$ GPa, $E_c = 380$ GPa, $\nu = 0.3$, $\alpha = 0$ [Present]

In order to obtain the outcomes and various conditions, the nondimensional critical buckling load is defined as $\lambda_c = N_x/E_c h$, and table 8 is employed to achieve this purpose.

Figures 2(a) and (b) show the accuracy of the proposed solution functions for thickness variations with change in nonlocal parameter (figure 2(a)) and porosity factor (figure 2(b)). It can be seen that by increasing nonlocal parameter the outcomes of the functions are decreased remarkably and reached to one another. In other words, for high values of small-scale parameter the proposed functions are more appropriate than lower values of ones. Furthermore, by investigation of figure 2(b), it is seen that for various values of porosity factor the presented functions are suitable ones and there is no difference in the results.

To investigate both porosity cases and also both analytic approaches, figures 3(a) and (b) are considered whilst the thickness to length ratio is the changeable factor. In the first figure, by comparing three states; evenly porosity (*P-I*), unevenly porosity (*P-II*) and non-porosity (prefect) FG nanoplates, it is clear that when the plate has unevenly and miscellaneous cavities in its volume the plate's critical buckling loads are noticeably nearer to prefect plates. As a rule, in such a condition we can ignore porosity in analyzing of stability of FGMs. It also demonstrates that by increasing the span ratio (h/L_x), all of the states are getting closer and closer to one another. It can be concluded that in large values of span ratio, there is no need to analyze porosity in buckling of moderately thick and thick plates. In fact, porosity in this condition is not an important factor. From figure 3(b) it is depicted that both analytical solutions are in an excellent agreement and there is no difference between their results. Although the increase of the span

M Malikan *et al*

Table 3. Comparison of buckling factors, $\lambda = N_x Ly^2 h/\pi^2 D$ of the biaxially compressed rectangular plates.

		Thickness to width ratio, h/Ly								
		0.05			0.10			0.15		
Boundary conditions	Aspect ratio (Lx/Ly) Grid size, $X \times Y \times Z$	[85] 3D, HDQ DQ	[86] Mindlin, Pb-Ritz method	Present, 3D	[85] 3D, HDQ DQ	[86] Mindlin, Pb-Ritz method	Present, 3D	[85] 3D, HDQ DQ	[86] Mindlin, Pb-Ritz method	Present, 3D
SSSS	0.5	4.6486 4.7919	4.8277	4.7731	4.2402 4.2729	4.3754	4.2849	3.6294 3.6298	3.7844	3.6101
	1.0	1.8194 1.9657	1.9719	1.9787	1.8355 1.8706	1.8920	1.8639	1.7191 1.7338	1.7723	1.7363
	1.5	1.2795 1.4265	1.4297	1.4231	1.3398 1.3755	1.3872	1.3620	1.2843 1.2994	1.3218	1.2949

*The results for HDQ and DQ are in convergence values.

Table 4. Comparison study of the critical buckling load parameter ($\lambda = N_x Ly^2/\pi^2 D$) of isotropic square plate under uniaxial load.

References	h/L_x		
	0.05	0.1	0.2
[87], FSDT-DQ	3.9444	3.7865	3.2637
[88], Mindlin, Pb-Ritz method	3.944	3.786	3.264
Present- $Z_1(z)$	3.9061	3.7060	3.0929

Table 5. Comparison study of the critical buckling load parameter ($\lambda = N_x/E_c h$) for simply-supported square Al/Al$_2$O$_3$ FG plate under uniaxial load.

References	$h/L_x = 0.1$				$h/L_x = 0.2$			
	$k = 0$	$k = 0.5$	$k = 1$	$k = 4$	$k = 0$	$k = 0.5$	$k = 1$	$k = 4$
[87], FSDT-DQM	0.034 22	0.022 33	0.017 23	0.011 63	0.1180	0.078 10	0.060 66	0.040 23
[88], Navier	0.033 81	0.02214	0.01698	0.01131	0.1140	0.075 71	0.058 26	0.037 21
Present- $Z_1(z)$	0.034 02	0.022 44	0.017 12	0.011 42	0.1206	0.077 65	0.060 25	0.041 67

Table 6. Comparison of critical buckling loads (MN/m) for the FG plates with all edges simply-supported boundary conditions.

References	Loading	$k = 0$		$k = 1$	
		L_x/L_y		L_x/L_y	
		1	1.5	1	1.5
[90], HSDT-Levy solution	Uniaxial	1437.361	1527.903	702.304	748.920
	Biaxial	718.692	526.861	351.124	256.776
[91], HSDT-Navier solution	Uniaxial	1431.594	1519.588	700.068	745.801
	Biaxial	715.808	525.308	350.034	256.194
Present- $Z_1(z)$	Uniaxial	1447.6	1536.733	705.34	747.476
	Biaxial	723.797	530.629	349.67	256.189

Table 7. Comparison of nondimensional critical buckling loads ($\lambda = N_x L_x^2/E_m h^3$) for square FG plates with all edges simply-supported boundary conditions.

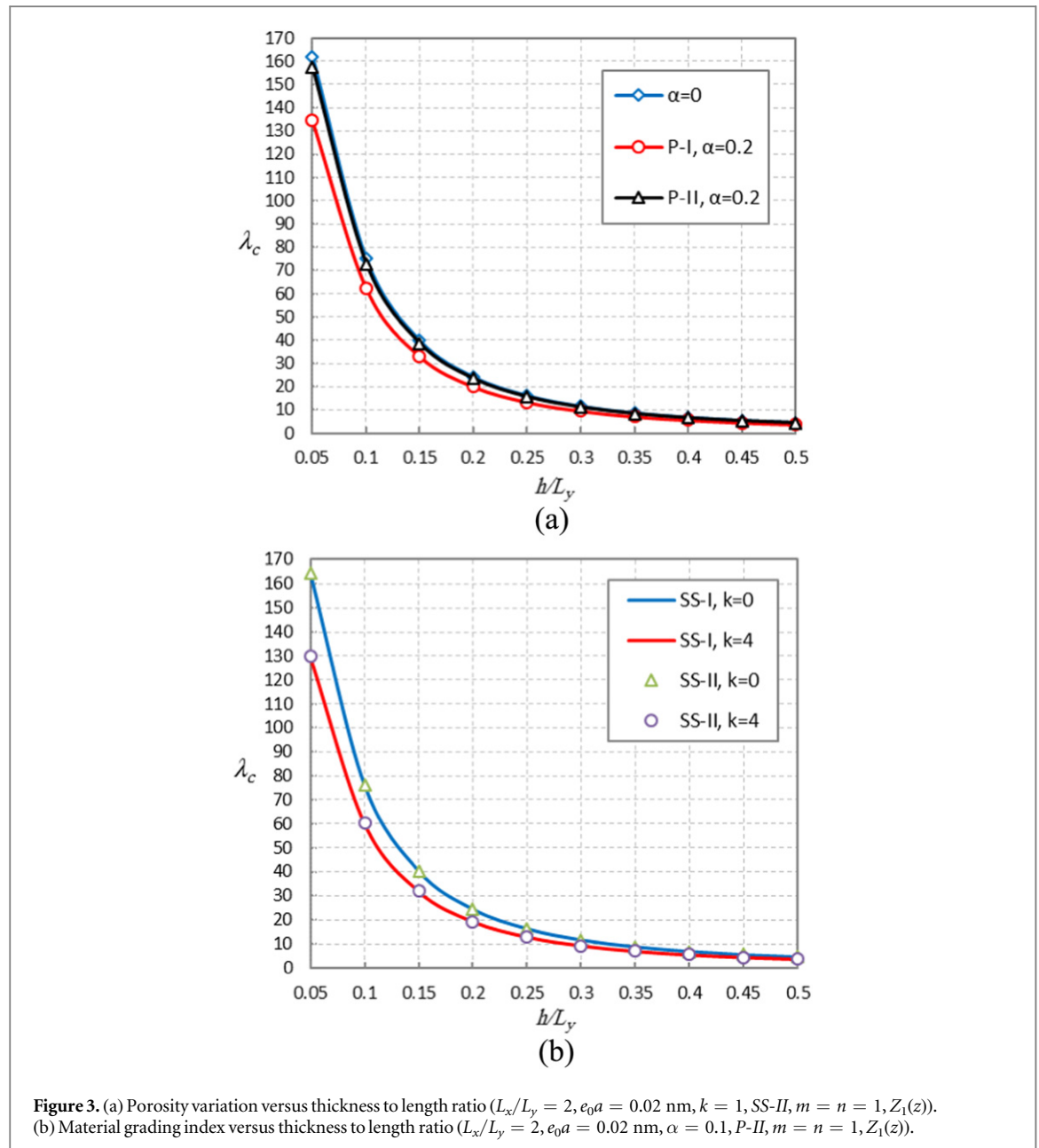| References	Loading	L_x/h	k					
			0	0.5	1	2	5	10
[16], TSDT-Levy solution	Uniaxial	5	16.0211	10.6254	8.2245	6.3432	7.5778	4.4807
		10	18.5785	12.1229	9.3391	7.2631	6.0353	5.4528
		20	19.3528	12.5668	9.6675	7.5371	6.3448	5.7668
		100	19.6145	12.7158	9.7775	7.6293	6.4507	5.8752
	Biaxial	5	8.0105	5.3127	4.1122	3.1716	2.5265	2.2403
		10	9.2893	6.0615	4.6695	3.6315	3.0177	2.7264
		20	9.6764	6.2834	4.8337	3.7686	3.1724	2.8834
		100	9.8073	6.3579	4.8888	3.8147	3.2254	2.9376
Present- $Z_1(z)$	Uniaxial	5	16.1172	10.6838	8.2656	6.3685	7.6043	4.4896
		10	18.6528	12.1653	9.3671	7.2776	6.0443	5.4582
		20	19.3915	12.5856	9.6771	7.5431	6.3492	5.7696
		100	19.6243	12.7208	9.7804	7.6308	6.4516	5.8753
	Biaxial	5	8.0345	5.3259	4.1204	3.1763	2.5297	2.2425
		10	9.3078	6.0718	4.6765	3.6351	3.0201	2.7277
		20	9.6860	6.2877	4.8366	3.7701	3.1733	2.8839
		100	9.8082	6.3584	4.8890	3.8148	3.2255	2.9376
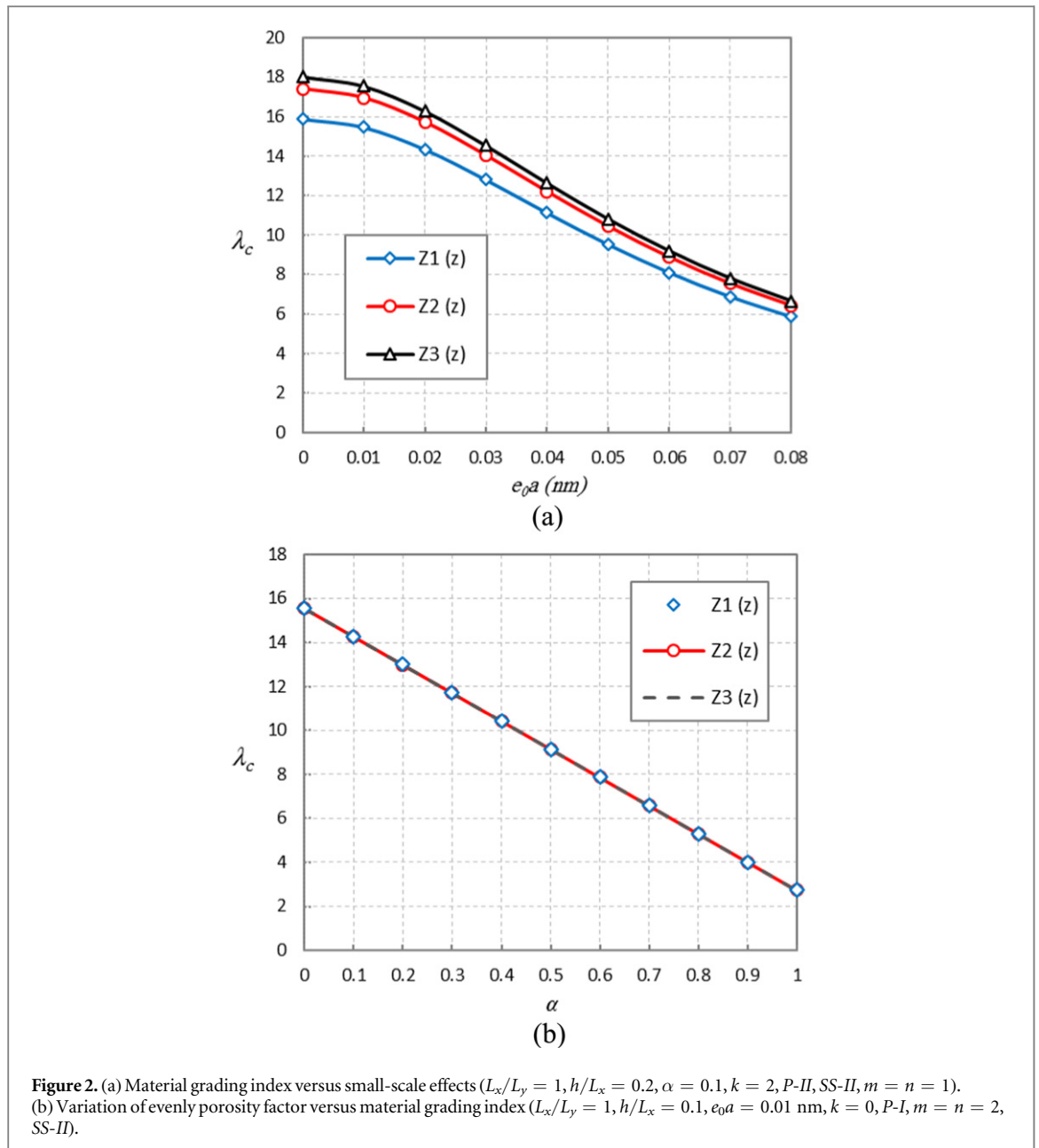
Figure 2. (a) Material grading index versus small-scale effects ($L_x/L_y = 1, h/L_x = 0.2, \alpha = 0.1, k = 2, P\text{-}II, SS\text{-}II, m = n = 1$). (b) Variation of evenly porosity factor versus material grading index ($L_x/L_y = 1, h/L_x = 0.1, e_0 a = 0.01$ nm, $k = 0, P\text{-}I, m = n = 2, SS\text{-}II$).

Table 8. Material properties of the FG porous nanoplate used in this paper as follows:.

	Material	Elastic properties
FG porous nanoplates ($\nu = 0.3$) [92–94]	Porous metal; stainless steel-grade 304 (SUS304)	$E_m = 201.04$ GPa
	Nano-oxide ceramic; silicon nitride (Si$_3$N$_4$)	$E_c = 310$ GPa

ratio shows that in high amounts of it, there is no need to consider the nanoplate as a FGM due to equaling results of FGM and non-FGM, this might not be a sensible conclusion in physical interpretation.

Variation of nonlocal parameter for both analytical solutions versus grading index (figure 4(a)) and porosities (figure 4(b)) has been plotted. In both figures the analytical solutions are completely corresponded to each other. Although the figures represent that by increasing nonlocal parameter the results of various cases have become closer to one another, the significant harvest can be the impact of small-scale parameter on the results of critical buckling loads of the FG nanoplate. Because, low values of this parameter decrease the buckling loads remarkably.

Figure 3. (a) Porosity variation versus thickness to length ratio ($L_x/L_y = 2, e_0 a = 0.02$ nm, $k = 1, SS\text{-}II, m = n = 1, Z_1(z)$).
(b) Material grading index versus thickness to length ratio ($L_x/L_y = 2, e_0 a = 0.02$ nm, $\alpha = 0.1, P\text{-}II, m = n = 1, Z_1(z)$).

To further examine the porosities, figure 5(a) is shown for evenly porosity and figure 5(b) is revealed for unevenly porosity which both are considered for same grading indexes. In the first observation, it can be evident that the evenly porosity is further impressive for the FG nanoplate in light of the slope of curves on the diagrams. In fact, the decrease of buckling loads by using evenly porosity is much more than decrease of buckling loads by applying unevenly porosity parameter. It can be stated that the use of the evenly porosity leads to a softer plate. In addition, it is clearly seen that k factor has not influenced on the porosities. Since the distances between the curves of various power law index in both figures are intensively similar to each other. By more examining, it is deduced that results of critical buckling loads decreased linearly with an increase in porosities.

Figures 6(a) and (b) show variation of material grading index versus evenly porosity and half-waves, respectively. It can be seen from figure 6(a) that the increase of grading index decreases critical buckling loads nonlinearly. However, after $k = 4$, this decreasing trend has more intensity and finally for $k \to \infty$ which the FG nanoplate is converted to fully metal, the results of critical buckling loads would be smaller. This nonlinear trend is accompanied with linear decreasing trend of porosity in figure 6(c). In this figure, in the right section the changes in porosity and in the left section the variation of grading index are illustrated. According to this three-dimensional figure, it can be deduced that the lowest buckling loads when $0.2 \leqslant \alpha \leqslant 0.6$ and $k = 5$ occurs. Moreover, a comparison between results of half-waves is presented by
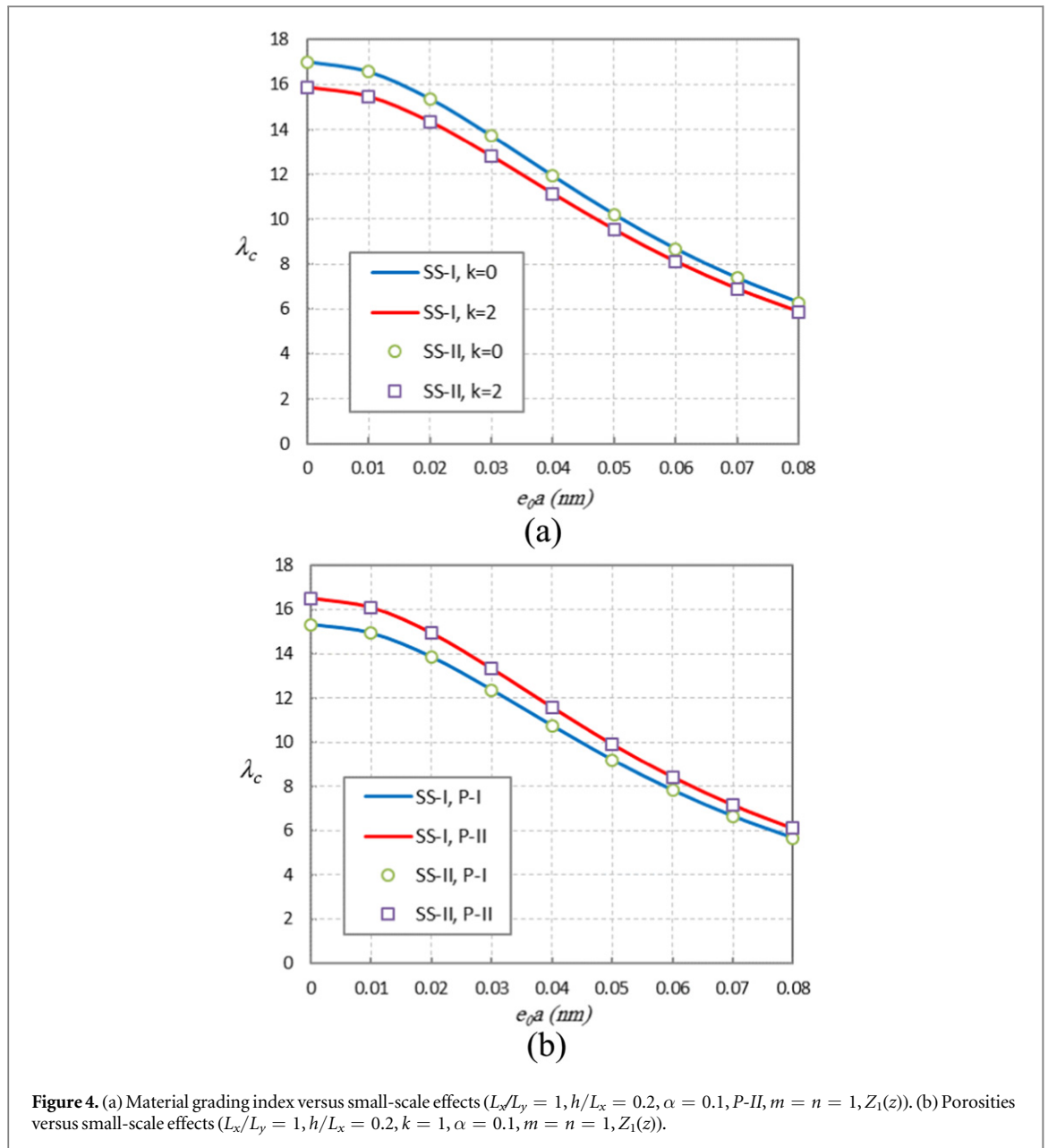
Figure 4. (a) Material grading index versus small-scale effects ($L_x/L_y = 1, h/L_x = 0.2, \alpha = 0.1, P\text{-}II, m = n = 1, Z_1(z)$). (b) Porosities versus small-scale effects ($L_x/L_y = 1, h/L_x = 0.2, k = 1, \alpha = 0.1, m = n = 1, Z_1(z)$).

figure 6(b) within which both type of porosities are considered. It is indicated that for lower half-waves the decreasing trend of buckling loads which resulted from increasing grading index is slower than higher half-waves. It can be seen after a specific value of k, the results of various half-waves tend to be equal to one another.

By utilizing figure 7 the changes in aspect ratio (L_x/L_y) in the right section and also span ratio (h/L_x) in the left section of figure are shown. The increase of aspect ratio leads to growing the resistance of the FG nanoplate linearly, however, the span ratio is a more important factor due to its very smaller values.

5. Conclusions

The constitutive equations for a porous functionally graded material were derived in Cartesian coordinate system using three-dimensional elasticity theory. The governing equations were in a nonlocal form by using nonlocal elasticity theory of Eringen. In order for results to be obtained, the nonlocal governing equations were solved with the volume integral methods in which some shape functions were assumed. After comparing the results of the present solution with other research results, the excellent agreements were observed. Thereafter,
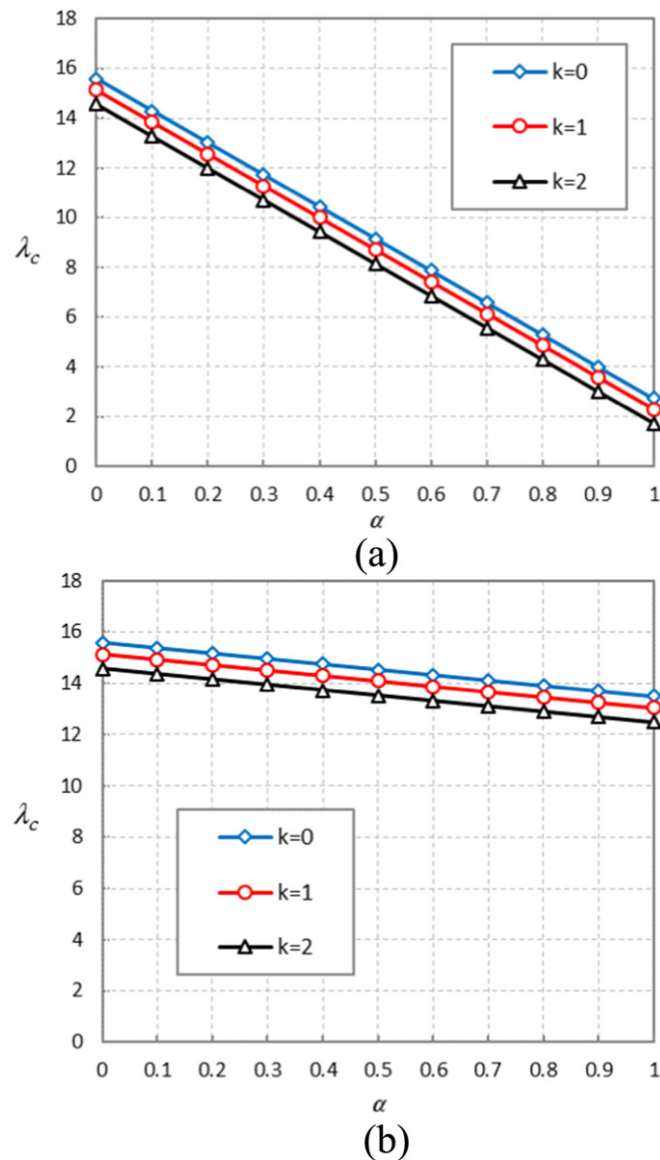
Figure 5. (a) Variation of evenly porosity factor versus material grading index ($L_x/L_y = 1$, $h/L_x = 0.1$, $e_0 a = 0.01$ nm, *P-I*, $m = n = 2$, $Z_1(z)$, *SS-II*). (b) Variation of unevenly porosity factor versus material grading index ($L_x/L_y = 1$, $h/L_x = 0.1$, $e_0 a = 0.01$ nm, *P-II*, $m = n = 2$, $Z_1(z)$, *SS-II*).

with utilizing some significant parameters the diagrams were plotted within which some noticeable conclusions are presented as follows:

- Even porosity made plates softer and results of uneven porosity are so close to the prefect material which led to this considerable conclusion that porosity as an uneven distribution cannot be important in order to implement it in the equations.

- The drastic influence of three-dimensional nonlocal parameter on the critical buckling analysis of FG nanoplate proved that this parameter plays a determinative role to examine mechanical behavior of porous FG nanoplates.
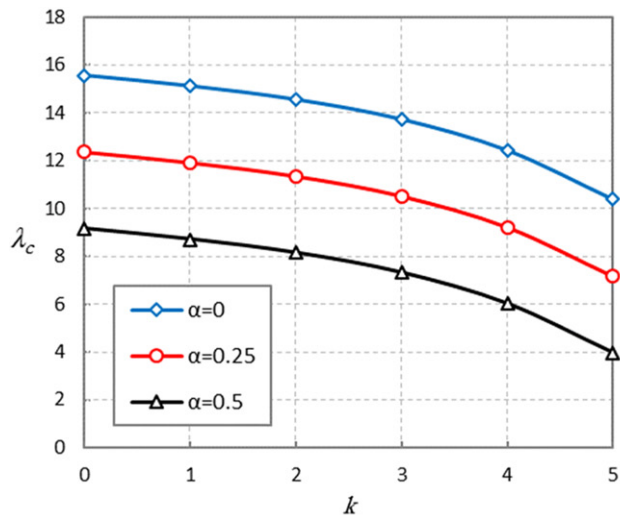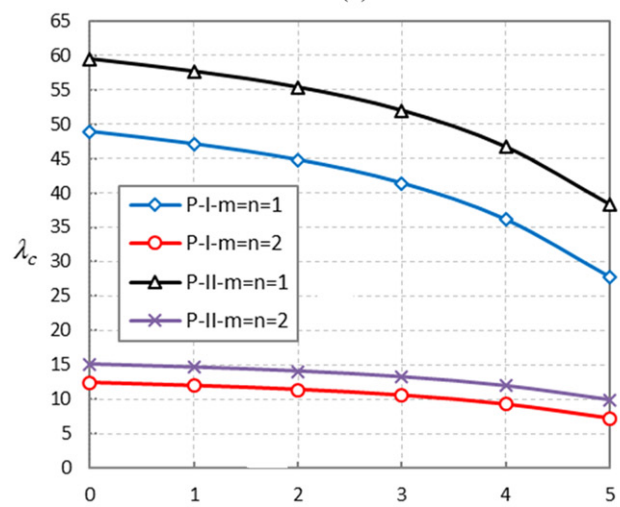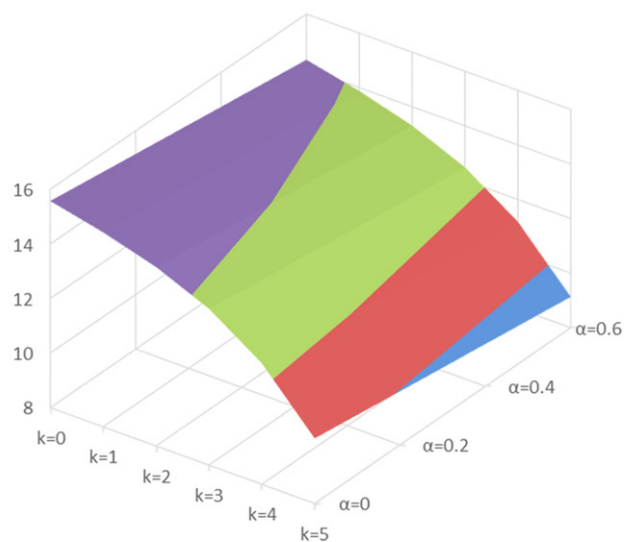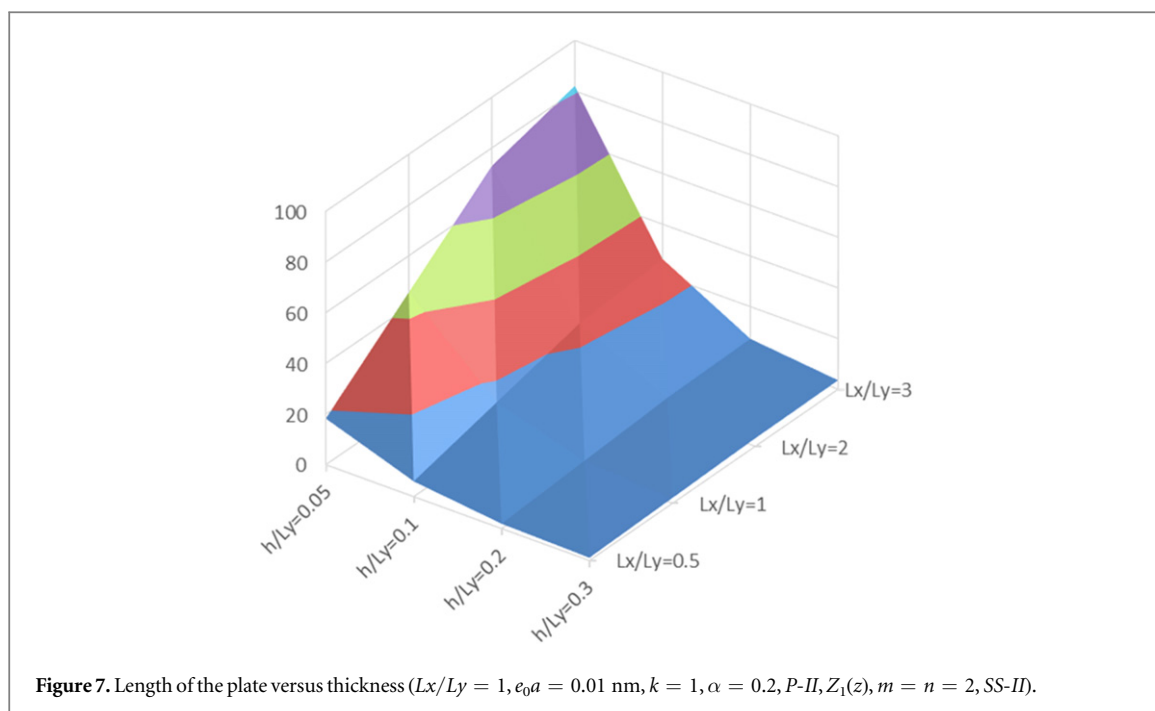
Figure 6. (a) Material grading index versus porosity factor variation ($L_x/L_y = 1$, $h/L_x = 0.1$, $e_0a = 0.01$ nm, P-I, $m = n = 2$, $Z_1(z)$, SS-II). (b) Material grading index versus porosity factors ($L_x/L_y = 1$, $h/L_x = 0.1$, $\alpha = 0.25$, P-I, $e_0a = 0.01$ nm, $Z_1(z)$, SS-II). (c) Material grading index versus porosity factors ($Lx/Ly = 1$, $h/Lx = 0.1$, $e_0a = 0.01$ nm, $Z_1(z)$, P-II, $m = n = 2$, SS-II).

Figure 7. Length of the plate versus thickness ($Lx/Ly = 1$, $e_0a = 0.01$ nm, $k = 1$, $\alpha = 0.2$, $P\text{-}II$, $Z_1(z)$, $m = n = 2$, $SS\text{-}II$).

ORCID iDs

Mohammad Malikan ⓘ https://orcid.org/0000-0001-7356-2168
Francesco Tornabene ⓘ https://orcid.org/0000-0002-5968-3382
Rossana Dimitri ⓘ https://orcid.org/0000-0001-7153-4307

References

[1] Vuong Nguyen V D, Tran M-T and Lee C-H 2018 Nonlinear thermal buckling analyses of functionally graded plates by a mesh-free radial point interpolation method *Eng. Anal. Bound. Elem.* **87** 153–64

[2] Lieu Q X, Lee S, Kang J and Lee J 2018 Bending and free vibration analyses of in-plane bi-directional functionally graded plates with variable thickness using isogeometric analysis *Compos. Struct.* **92** 434–51

[3] Thai H-T and Kim S-E 2013 A simple higher-order shear deformation theory for bending and free vibration analysis of functionally graded plates *Compos. Struct.* **96** 165–73

[4] Fakhari V, Ohadi A and Yousefian P 2011 Nonlinear free and forced vibration behavior of functionally graded plate with piezoelectric layers in thermal environment *Compos. Struct.* **93** 2310–21

[5] Zenkour A M and Radwan A F 2018 Compressive study of functionally graded plates resting on Winkler–Pasternak foundations under various boundary conditions using hyperbolic shear deformation theory *Archive of Civil and Mechanical Engineering* **18** 645–58

[6] Thai H-T and Vo T-P 2013 A new sinusoidal shear deformation theory for bending, buckling, and vibration of functionally graded plates *Appl. Math. Modelling* **37** 3269–81

[7] Chu F, He J, Wang L and Zhong Z 2016 Buckling analysis of functionally graded thin plate with in-plane material inhomogeneity *Eng. Anal. Bound. Elem.* **65** 112–25

[8] Thai H-T and Kim S-E 2013 Closed-form solution for buckling analysis of thick functionally graded plates on elastic foundation *Int. J. Mech. Sci.* **75** 34–44

[9] Bever M B and Duwez P E 1972 Gradients in composite materials *Materials Science Engineering* **10** 1–8

[10] Carrera E, Brischetto S, Cinefra M and Soave M 2011 Effects of thickness stretching in functionally graded plates and shells *Composite Part-B Engineering* **42** 123–33

[11] Bousahla A A, Benyoucef S, Tounsi A and Hassan S 2016 On thermal stability of plates with functionally graded coefficient of thermal expansion *Struct. Eng. Mech.* **60** 313–35

[12] Akavci S S 2016 Mechanical behavior of functionally graded sandwich plates on elastic foundation *Composites Part B: Engineering* **96** 136–52

[13] Bouderba B, Ahmed H M S, Tounsi A and Hassan S 2016 Thermal stability of functionally graded sandwich plates using a simple shear deformation theory *Struct. Eng. Mech.* **58** 397–422

[14] Ghadiri M, Shafiei N and Babaei R 2017 Vibration of a rotary FG plate with consideration of thermal and Coriolis effects *Steel and Composite Structures* **25** 197–207

[15] El-Haina F, Bakora A, Boushala A A, Tounsi A and Hassan S 2017 A simple analytical approach for thermal buckling of thick functionally graded sandwich plates *Struct. Eng. Mech.* **63** 585–95

[16] Hichem B, Bakora A, Tounsi A, Boushala A A and Hassan S 2017 An efficient and simple four variable refined plate theory for buckling analysis of functionally graded plates *Steel and Composite Structures* **25** 257–70

[17] Zhang L, Liu J, Fang X and Nie G 2014 Effects of surface piezoelectricity and nonlocal scale on wave propagation in piezoelectric nanoplates *European Journal of Mechanics-A/Solids* **46** 22–9

[18] Li L, Hu Y and Ling L 2015 Flexural wave propagation in small-scaled functionally graded beams via a nonlocal strain gradient theory *Compos. Struct.* **133** 1079–92

[19] Shahsavari D and Janghorban M 2017 Bending and shearing responses for dynamic analysis of single-layer graphene sheets under moving load *Journal of the Brazilian Society of Mechanical Sciences and Engineering* **39** 3849–61

[20] Hichem B, Benrahou K H, Bousahla A A, Tounsi A and Hassan S 2017 A nonlocal zeroth-order shear deformation theory for nonlinear postbuckling of nanobeams *Struct. Eng. Mech.* **62** 695–702

[21] Zeighampour H, Beni Y T and Karimipour I 2017 Wave propagation in double-walled carbon nanotube conveying fluid considering slip boundary condition and shell model based on nonlocal strain gradient theory *Microfluidics and Nanofluidics* **21** 85

[22] Karami B, Janghorban M and Tounsi A 2018 Variational approach for wave dispersion in anisotropic doubly-curved nanoshells based on a new nonlocal strain gradient higher order shell theory *Thin-Walled Struct.* **129** 251–64

[23] Karami B, Janghorban M and Tounsi A 2018 Nonlocal strain gradient 3D elasticity theory for anisotropic spherical nanoparticles *Steel and Composite Structures* **27** 201–16

[24] Ebrahimi F and Salari E 2015 Thermal buckling and free vibration analysis of size dependent Timoshenko FG nanobeams in thermal environments *Compos. Struct.* **128** 363–80

[25] Shojaeian M, Tadi Beni Y and Ataei H 2016 Electromechanical buckling of functionally graded electrostatic nanobridges using strain gradient theory *Acta Astronaut.* **118** 62–71

[26] Zamani Nejad M, Hadi A and Rastgoo A 2016 Buckling analysis of arbitrary two-directional functionally graded Euler–Bernoulli nano-beams based on nonlocal elasticity theory *Int. J. Eng. Sci.* **103** 1–10

[27] Wu H, Kitipornchai S and Yang J 2017 Thermal buckling and postbuckling of functionally graded graphene nanocomposite plates *Mater. Des.* **132** 430–41

[28] Hosseini-Hashemi S, Rokni Damavandi Taher H, Akhavan H and Omidi M 2010 Free vibration of functionally graded rectangular plates using first-order shear deformation plate theory *Appl. Math. Modelling* **34** 1276–91

[29] Kar V R, Panda S K and Mahapatra T R 2016 Thermal buckling behaviour of shear deformable functionally graded single/doubly curved shell panel with TD and TID properties *Advances in Materials Research* **5** 205–21

[30] Meziane M A A, Abdelaziz H H and Tounsi A 2017 An efficient hyperbolic shear deformation theory for bending, buckling and free vibration of FGM sandwich plates with various boundary conditions *Steel and Composite Structures* **25** 693–704

[31] Malikan M, Jabbarzadeh M and Dastjerdi S 2017 Non-linear Static stability of bi-layer carbon nanosheets resting on an elastic matrix under various types of in-plane shearing loads in thermo-elasticity using nonlocal continuum *Microsyst. Technol.* **23** 2973–91

[32] Malikan M 2017 Electro-mechanical shear buckling of piezoelectric nanoplate using modified couple stress theory based on simplified first order shear deformation theory *Appl. Math. Modelling* **48** 196–207

[33] Malikan M 2017 Analytical predictions for the buckling of a nanoplate subjected to nonuniform compression based on the four-variable plate theory *Journal of Applied and Computational Mechanics* **3** 218–28

[34] Malikan M 2018 Buckling analysis of a micro composite plate with nano coating based on the modified couple stress theory *Journal of Applied and Computational Mechanics* **4** 1–15

[35] Malikan M 2018 Temperature influences on shear stability of a nanosize plate with piezoelectricity effect *Multidiscipline Modeling in Materials and Structures* **14** 125–42

[36] Golmakani M E, Malikan M, Sadraee Far M N and Majidi H R 2018 Bending and buckling formulation of graphene sheets based on nonlocal simple first order shear deformation theory *Mater. Res. Express* **5** 065010

[37] Malikan M and Sadraee Far M N 2018 Differential quadrature method for dynamic buckling of graphene sheet coupled by a viscoelastic medium using neperian frequency based on nonlocal elasticity theory *Journal of Applied and Computational Mechanics* **4** 147–60

[38] Malikan M and Nguyen V B 2018 Buckling analysis of piezo-magnetoelectric nanoplates in hygrothermal environment based on a novel one variable plate theory combining with higher-order nonlocal strain gradient theory *Physica E: Low-dimensional Systems and Nanostructures* **102** 8–28

[39] Malikan M, Nguyen V B and Tornabene F 2018 Damped forced vibration analysis of single-walled carbon nanotubes resting on viscoelastic foundation in thermal environment using nonlocal strain gradient theory *Engineering Science and Technology, an International Journal* (https://doi.org/10.1016/j.jestch.2018.06.001)

[40] Malikan M, Nguyen V B and Tornabene F 2018 Electromagnetic forced vibrations of composite nanoplates using nonlocal strain gradient theory *Mater. Res. Express* **5** 075031

[41] Tornabene F, Viola E and Inman D J 2009 2D Differential Quadrature solution for vibration analysis of functionally graded conical, cylindrical shell and annular plate structures *J. Sound Vib.* **328** 259–90

[42] Tornabene F, Fantuzzi N, Viola E and Batra R C 2015 Stress and strain recovery for functionally graded free-form and doubly-curved sandwich shells using higher-order equivalent single layer theory *Compos. Struct.* **119** 67–89

[43] Tornabene F, Fantuzzi N and Bacciocchi M 2014 Free vibrations of free-form doubly-curved shells made of functionally graded materials using higher-order equivalent single layer theories *Composites Part B: Engineering* **67** 490–509

[44] Tornabene F and Viola E 2013 Static analysis of functionally graded doubly-curved shells and panels of revolution *Meccanica* **48** 901–30

[45] Fantuzzi N, Tornabene F and Viola E 2016 Four-parameter functionally graded cracked plates of arbitrary shape: a GDQFEM solution for free vibrations *Mechanics of Advanced Materials and Structures* **23** 89–107

[46] Fantuzzi N, Tornabene F, Bacciocchi M and Dimitri R 2017 Free vibration analysis of arbitrarily shaped functionally graded carbon nanotube-reinforced plates *Composites Part B: Engineering* **115** 384

[47] Kamarian S, Salim M, Dimitri R and Tornabene F 2016 Free vibration analysis of conical shells reinforced with agglomerated carbon nanotubes *Int. J. Mech. Sci.* **108** 157–65

[48] Fantuzzi N, Brischetto S, Tornabene F and Viola E 2016 2D and 3D shell models for the free vibration investigation of functionally graded cylindrical and spherical panels *Compos. Struct.* **154** 573–90

[49] Kandasamy R, Dimitri R and Tornabene F 2016 Numerical study on the free vibration and thermal buckling behaviour of moderately thick functionally graded structures in thermal environments *Compos. Struct.* **157** 207–21

[50] Tornabene F, Brischetto S, Fantuzzi N and Bacciocchi M 2016 Boundary conditions in 2D numerical and 3D exact models for cylindrical bending analysis of functionally graded structures *Shock and Vibration* **2016** 1–17

[51] Nejati M, Asanjarani A, Dimitri R and Tornabene F 2017 Static and free vibration analysis of functionally graded conical shells reinforced by carbon nanotubes *Int. J. Mech. Sci.* **130** 383–98

[52] Jouneghani F Z, Dimitri R, Bacciocchi M and Tornabene F 2017 Free vibration analysis of functionally graded porous doubly-curved shells based on the first-order shear deformation theory *Applied Sciences* **7** 1–20

[53] Nejati M, Dimitri R, Tornabene F and Yas M H 2017 Thermal buckling of nanocomposite stiffened cylindrical shells reinforced by functionally graded wavy carbon nano-tubes with temperature-dependent properties *Applied Sciences* **7** 1–24

[54] Jouneghani F Z, Dimitri R and Tornabene F 2018 Structural response of porous FG nanobeams under hygro-thermo-mechanical loadings *Composites Part B: Engineering* **152** 71–8

[55] Kiani Y, Dimitri R and Tornabene F 2018 Free vibration study of composite conical panels reinforced with FG-CNTs *Engineering Structures* **172** 472–82

[56] Arefi M, Mohammadi M, Tabatabaeian A, Dimitri R and Tornabene F 2018 Two-dimensional thermo-elastic static analysis of FG-CNTRC cylindrical pressure vessels *Steel and Composite Structures* **27** 525–36

[57] Kiani Y, Dimitri R and Tornabene F 2018 Free vibration of FG-CNT reinforced composite skew cylindrical shells using chebyshev-ritz formulation *Composites Part B: Engineering* **147** 169–77

[58] She G L, Shu X and Ren Y R 2016 Thermal buckling and postbuckling analysis of piezoelectric FGM beams based on high-order shear deformation theory *J. Therm. Stresses* **40** 783–97

[59] She G L, Yuan F G and Ren Y R 2017 Nonlinear analysis of bending, thermal buckling and post-buckling for functionally graded tubes by using a refined beam theory *Compos. Struct.* **165** 74–82

[60] She G L, Yuan F G and Ren Y R 2017 Research on nonlinear bending behaviors of FGM infinite cylindrical shallow shells resting on elastic foundations in thermal environments *Compos. Struct.* **170** 111–21

[61] She G L, Yuan F G, Ren Y R and Xiao W S 2017 On buckling and postbuckling behavior of nanotubes *Int. J. Eng. Sci.* **121** 130–42

[62] She G L, Ren Y R, Yuan F G and Xiao W S 2018 On vibrations of porous nanotubes *Int. J. Eng. Sci.* **125** 23–35

[63] She G L and Ren F G 2018 One wave propagation of porous nanotubes *Int. J. Eng. Sci.* **130** 62–74

[64] She G L, Ren Y R, Xiao W S and Liu H B 2018 Study on thermal buckling and post-buckling behaviors of FGM tubes resting on elastic foundations *Structural Engineering & Mechanics* **66** 729–36

[65] Sun M-H *et al* 2016 Applications of hierarchically structured porous materials from energy storage and conversion, catalysis, photocatalysis, adsorption, separation, and sensing to biomedicine *Chem. Soc. Rev.* **45** 3479–563

[66] Lu G-Q and Zhao X-S 2004 *Nanoporous Materials: Science and Engineering* (UK: Imperial College Press) (https://doi.org/10.1142/p181)

[67] Polarz S and Smarsly B 2002 Nanoporous materials *J. Nanosci. Nanotechnol.* **2** 581–612

[68] Zabukovec Logar N and Kaučič V 2006 Nanoporous materials: from catalysis and hydrogen storage to wastewater treatment *Acta Chimica Slovenica* **53** 117–35 http://www.worldcat.org/oclc/440034476

[69] Shafiei N and Kazemi M 2017 Nonlinear buckling of functionally graded nano-/micro-scaled porous beams *Compos. Struct.* **178** 483–92

[70] Wang Y-Q and Zu J-W 2017 Vibration behaviors of functionally graded rectangular plates with porosities and moving in thermal environment *Aerospace Science and Technology* **69** 550–62

[71] Wang Y-Q 2018 Electro-mechanical vibration analysis of functionally graded piezoelectric porous plates in the translation state *Acta Astronaut.* **143** 263–71

[72] Ansari R, Shahabodini A and Shojaei M F 2016 Nonlocal three-dimensional theory of elasticity with application to free vibration of functionally graded nanoplates on elastic foundations *Physica E: Low-dimensional Systems and Nanostructures* **76** 70–81

[73] Brischetto S 2017 Exact three-dimensional static analysis of single- and multi-layered plates and shells *Composites Part B: Engineering* **119** 230–52

[74] Ansari R, Faghih Shojaei M, Shahabodini A and Bazdid-Vahdati M 2015 Three-dimensional bending and vibration analysis of functionally graded nanoplates by a novel differential quadrature-based approach *Compos. Struct.* **131** 753–64

[75] Dastjerdi S and Akgöz B 2018 New static and dynamic analyses of macro and nano FGM plates using exact three-dimensional elasticity in thermal environment *Compos. Struct.* **192** 626–41

[76] Salehipour H, Nahvi H, Shahidi A R and Mirdamadi H R 2017 3D elasticity analytical solution for bending of FG micro/nanoplates resting on elastic foundation using modified couple stress theory *Appl. Math. Modelling* **47** 174–88

[77] Alibeigloo A 2017 Three dimensional coupled thermoelasticity solution of sandwich plate with FGM core under thermal shock *Compos. Struct.* **177** 96–103

[78] Lomte Patil Y T, Kant T and Desai Y M 2018 Comparison of three dimensional elasticity solutions for functionally graded plates *Compos. Struct.* (https://doi.org/10.1016/j.compstruct.2018.02.051)

[79] Wattanasakulpong N and Chaikittiratana A 2015 Flexural vibration of imperfect functionally graded beams based on Timoshenko beam theory: Chebyshev collocation method *Meccanica* **50** 1331–42

[80] Pham H C, Trinh M C, Nguyen D K and Nguyen D D 2018 Nonlinear thermomechanical buckling and post-buckling response of porous FGM plates using Reddy's HSDT *Aerospace Science and Technology* **77** 419–28

[81] She G-L, Yuan F-G and Ren Y-R 2017 Thermal buckling and post-buckling analysis of functionally graded beams based on a general higher-order shear deformation theory *Appl. Math. Modelling* **47** 340–57

[82] Eringen A C and Nonlocal A 1983 Finite element approach to nano beams *J. Appl. Phys.* **54** 4703–10

[83] Eringen A C 2002 *Nonlocal Continuum Field Theories* (New York: Springer) (https://doi.org/10.1007/b97697)

[84] Salehipour H, Nahvi H and Shahidi A R 2015 Exact analytical solution for free vibration of functionally graded micro/nano plates via three dimensional nonlocal elasticity *Physica E: Low-dimensional Systems and Nanostructures* **66** 350–8

[85] Liew K-M, Teo T-M, Han J-B and Kitipornchai S 2001 Three-dimensional static solutions of rectangular plates by variant differential quadrature method *Int. J. Mech. Sci.* **43** 1611–28

[86] Wang C-M, Liew K-M, Xiang Y and Kitipornchai S 1993 Buckling of rectangular Mindlin plates with internal line supports *Int. J. Solids Struct.* **30** 1–17

[87] Malekzadeh P, Golbahar Haghighi M R and Beni A A 2012 Buckling analysis of functionally graded arbitrary straight-sided quadrilateral plates on elastic foundations *Meccanica* **47** 321–33

[88] Xiang Y 1993 Numerical developments in solving the buckling and vibration of Mindlin plates *PhD thesis* (https://doi.org/10.14264/uql.2015.571)The University of Queensland, Australia http://doi.org/10.14264/uql.2015.571

[89] Matsunaga H 2008 Free vibration and stability of functionally graded plates according to 2D higher-order deformation theory *Compos. Struct.* **82** 499–512

[90] Boudaghi M and Saidi A R 2010 Levy-type solution for buckling analysis of thick functionally graded rectangular plates based on the higher-order shear deformation plate theory *Appl. Math. Modelling* **34** 3659–73

[91] Abdollahi M, Saeedi A and Mohammadi M 2015 Buckling of thick functionally graded plates based on the higher order shear and normal deformation theories *Iranian J. Mech. Eng. Trans. ISME* **17** 86–105 http://jmep.isme.ir/article_25862_en.html

[92] Yang J and Shen H-S 2002 Vibration characteristics and transient response of shear-deformable functionally graded plates in thermal environments *J. Sound Vib.* **255** 579–602

[93] Ziaee S 2015 Small scale effect on linear vibration of buckled size-dependent FG nanobeams *Ain Shams Engineering Journal* **6** 587–98

[94] http://accuratus.com/silinit.html